PYROLYSIS KINETICS OF ETHYLENE-PROPYLENE (EPM) AND ETHYLENE-PROPYLENE-DIENE (EPDM)

Antonio Perejón, Pedro E. Sánchez-Jiménez, Eva Gil-González, Luis A. Pérez-Maqueda* and José M. Criado.

Instituto de Ciencia de Materiales de Sevilla, C.S.I.C.-Universidad de Sevilla, C. Américo Vespucio nº49, 41092 Sevilla, Spain.

Abstract

The thermal degradation kinetics of several ethylene-propylene copolymers (EPM) and ethylene-propylene-diene terpolymers (EPDM), with different chemical compositions, have been studied by means of the Combined Kinetic Analysis. Until now, attempts to establish the kinetic model for the process have been unsuccessful and previous reports suggest that a model other than a conventional *n*th order might be responsible. Here, a random scission kinetic model, based on the breakage and evaporation of cleavaged fragments, is found to describe the degradation of all compositions studied. The suitability of the kinetic parameters resulting from the analysis has been asserted by successfully reconstructing the experimental curves. Additionally, it has been shown that the activation energy for the pyrolysis of the EPM copolymers decreases by increasing the propylene content. An explanation for this behavior is given. A low dependence of the EPDM chemical composition on the activation energy for the pyrolysis has been reported, although the thermal stability is influenced by the composition of the diene used.

Keywords: EPDM; thermal degradation; kinetic model; random scission

* Corresponding author. Tel +34954489548 Fax +34954460665
e-mail address: maqueda@cica.es

1. Introduction

The ethylene-propylene-diene terpolymer (EPDM) is an elastomer based on the EPM copolymer, which consists of ethylene and propylene units as part of the main polymer chain. For the commercial preparation, a third diene co-monomer is included, introducing an unsaturation on a side chain to facilitate peroxide crosslinking reactions and to permit sulfur vulcanization [1]. The EPDM itself may vary in ethylene and propylene proportions, as well as in the amount and type of diene used. The vulcanization is possible because the non-conjugated diene is grafted onto the main polymer chain creating interchain sulfur cross-linking. EPDM has a relatively low unsaturation level and therefore requires complex cure systems to achieve the desired properties. Nearly every conceivable combination of curing ingredients has been evaluated in various EPDM polymers over the years [2, 3]. Vulcanized EPDM shows some interesting properties, such as ozone, heat, light, weathering and chemical resistance [4]. The EPDM blends have also been extensively studied, dealing with the synthesis, characterization and applications of these systems and their nanocomposites [5-11]. Moreover, it has been reported that the ethylene content influences the properties of the EPDM polymers [12], and that a higher ethylene content gives more green strength (high elongation in the uncured state), poorer low temperature properties, imparts a more crystalline nature to the EPDM and increases its glass transition temperature.

The main application of this material is in automotive industry because of its low cost, low specific density, ease of processability, paintability and weatherability. Another uses are as bumper fascias, grilles, wire and cable jacketing, air dams, rub strips, swim fins, handle grips and weatherstripping. Due to these applications, the degradation of

EPDM and its blends is a very important issue, and has been widely studied in the literature under diverse settings, i.e. oxidative degradation [13], artificial weathering environments [14], ultrasonic irradiation [15], photo-oxidation [16, 17], thermal degradation [12, 18-21], etc. However, only some of those previous works deal with the kinetics of thermal degradation of this material [12, 19, 22]. Moreover, the use of conventional n*th* order kinetic equations, commonly used for polymer thermal degradation processes, has proven unsuccessful for describing the thermal degradation of EPDM and it has been suggested that another, more complex, model should be used for describing the degradation. Gamlin *et al*, studying a set of isothermal curves suggested an Avrami-Erofeev nucleation and growth model [19]. So far, such model is not well established, so further investigation is necessary.

In recent works, it has been demonstrated that the thermal degradation of polymers may obey mechanisms other than n*th* order [23-27]. In these papers, the determination of the kinetics parameters was done from the study of curves obtained under different conditions and without the previous assumption of kinetic models.

The scope of this work is to study the pyrolysis kinetic mechanism of a set of EPM and EPDM samples supplied by the two most important industrial manufacturers of these products for industrial use. The knowledge of both the kinetic parameters and the kinetic model is very important in order to predict the burning behavior at different temperatures, which would be of crucial importance provided the massive use of EPDM as thermal and acoustic isolating of buildings.

2. Materials and Methods

The samples of EPDM and EPM studied are manufactured for industrial use and were supplied by ExxonMobil (Vistalon rubbers) and DSM Elastomers (named C2 EPM and EPDMs). The chemical composition of the different studied samples is included in Table 1. Thermogravimetric (TGA) measurements were performed in a TA Instruments Q5000 thermobalance (New Castle, DE, USA). Small pieces (~8mg) of the original samples were placed on a platinum pan. The experiments were recorded under linear heating, isothermal and controlled rate thermal analysis.

3. Theory

3.1 Theoretical background

The reaction rate, dα/dt, of a solid state reaction can be described by the following equation:

$$\frac{d\alpha}{dt} = A\exp\left(-Ea/RT\right)f\left(\alpha\right) \qquad (1),$$

Where *A* is the Arrhenius pre-exponential factor, *R* is the gas constant, *Ea* the apparent activation energy, α the reacted fraction, *T* is the process temperature and *f(α)* accounts for the reaction rate dependence on α. The kinetic model *f(α)*is an algebraic expression which is usually associated with a physical model that describes the kinetics of the solid state reaction. Table 1 lists the functions corresponding to the most commonly used mechanisms found in literature. The reacted fraction, α, can be expressed as defined below:

$$\alpha = \frac{w_0 - w}{w_0 - w_f} \qquad (2),$$

wherew_o is the initial mass, w_f the mass of residual char and w the sample mass at an instant t.

3.2 Isoconversional Analysis

Isoconversional methods, also known as "model-free", are used for determining the apparent activation energy as a function of the reacted fraction without any previous assumption on the kinetic model fitted by the reaction [28, 29]. The Friedman isoconversional method is a widely used differential method that, unlike conventional integral isoconversional methods, provides accurate values of the activation energies even if they were a function of the reacted fraction[30]. Eq. (1) can be written in logarithmic form:

$$\ln\left(\frac{d\alpha}{dt}\right) = \ln\left(Af(\alpha)\right) - \frac{Ea}{RT} \tag{3}$$

The activation energy at a constant α value can be determined from the slope of the plot of the left hand side of Eq. (3) against the reverse of the temperature, at constant values of α.

3.3 Combined Kinetic Analysis.

The logarithmic form of the general kinetic Eq. (1) can be rewritten as follows:

$$\ln\left(\frac{d\alpha/dt}{f(\alpha)}\right) = \ln A - \frac{Ea}{RT} \tag{4}$$

The plot of the left hand side of the equation versus the reverse of temperature will yield a straight line if the proper $f(\alpha)$ is considered for the analysis [31]. The apparent

activation energy can be calculated from the slope of such plot, while the intercept leads to the pre-exponential factor. As no assumption regarding the thermal pathway is made in Eq. (3), the kinetic parameters obtained should be independent of the thermal pathway. Thus, this method would allow for the simultaneous analysis of any set of experimental data obtained under different thermal schedules [32]. Recently, it has been reported that a modified Sestak and Berggren equation, i.e. $f(\alpha)=c\ \alpha^n\ (1-\alpha)^m$, with values for n and m in the range from 0.4 to 0.8 and -1 to 0.7, respectively, not only fits every kinetic ideal model proposed for solid state processes, but also accounts for the deviations of the ideal kinetic models due to, for example, inhomogeneities in particle size and shapes [32], what means that this equation behave as a umbrella, covering the whole set of kinetic equations describing solid state reactions. Thus, the use of this equation does not limit the kinetic analysis to the use of exclusively ideal kinetic models. This is especially important because if the kinetic model is discriminated from a predefined set of models, one of them would be selected as the "best model" even if the set does not contain the true one [33]. Also, it has been observed that deviations from the ideal situations assumed in the kinetic models change the form of the *f(α)*functions and consequently the experimental curves cannot be properly fitted by the theoretical *f(α)*functions.

Introducing the modified Sestak-Berggren equation in (4) we reach:

$$\ln\left(\frac{d\alpha/dt}{(1-\alpha)^n\,\alpha^m}\right)=\ln cA-Ea/RT \qquad (5)$$

The Pearson linear correlation coefficient between the left hand side of the equation and the reverse of the temperature is set as an objective function for optimization. By means of the maximize function of the software Mathcad, the parameters Ea, A, *n* and *m*

leading to the best linear correlation are determined from the simultaneous fitting of the whole set of α-T plots obtained under different heating schedules[32]. Nevertheless, it should be noted that the modified Sestak-Berggren equation is used here as a fitting function without physical meaning. Thus, the shape of the resulting Sestak-Berggren function with the *n* and *m* parameters obtained from the fitting should be compared with those of the function of the ideal kinetic models to determine the true kinetic model that describes the process.

4. Results and discussion

Figure 1 shows the thermal degradation curves of the different EPDM and EPM tested compositions (included in Table 1), all experiments were recorded at the same linear heating rate (5 K min^{-1}). Figure 1a includes the results for the EPDM samples whereas Figure 1b shows the results for EPM samples. Moreover, the temperatures corresponding to 10% (α=0.1) and 50% (α=0.5) degradation as obtained from Figure 1 have been included in Table 1 for the different compositions. For the EPM samples (Figure 1b, Table 1), the different structure produced by the different ethylene content of both samples plays a role in the thermal stability of the material, and the larger the ethylene contents the higher the degradation temperature, in agreement with previous reports [12]. For the EPDM samples, the situations seems to be a little more complex as samples differ in ethylene, propylene and diene contents as well as in the type of diene. Nevertheless, some trends can be found in the thermal behavior of those samples. Thus, compositions that include dicyclopentadiene (DCPD) are less stable than compositions with ethylidene norbornene (ENB). Moreover, the larger the DCPD content the lower the degradation temperature (Figure 1b, Table 1). Thus, the sample EPDM 58C2 (4.5%

DCPD) degrades at the lowest temperature followed by EPDM 67C2 (2% DCPD) and EPDM 64C2 (1% DCPD). Interestingly, sample EPDM 67 C2 has both DCPD and ENB diene groups, in such a way that the total amount of diene from both types of diene groups is larger than that of EPDM 67C2, but the thermal stability seems to be determined by the DCPD groups rather than by the ENB ones. For those compositions that include only ENB groups differences in stability are very small, but the degradation temperature is related with the total content of ethylene + diene groups, which is related to the content of propylene, independently of the origin or manufacturer of the sample. Thus, the larger the total amount of ethylene + diene groups, the higher the decomposition temperature, and the decomposition sequence from smaller to higher decomposition temperature is the following: Vistalon5601 < EPDM70C2 < Vistalon7001 < Vistalon7800.

A set of TGA curves was recorded under linear heating rate, isothermal and constant rate experimental conditions for every elastomer sample shown in Table 1. The collected experimental data were employed to perform a thorough kinetic analysis, including Friedman isoconversional and combined analysis methods, as described in the theoretical section. Given the amount of samples studied, for the sake of brevity, the kinetic analysis procedure is fully detailed exclusively for the degradation of the Vistalon7800. The results obtained for the rest of the elastomers, using the same analysis procedure, are included in Table 1. Figure 2 shows a set of experimental curves recorded under different linear heating rate (Figure 2a), isotherm (Figure 2b) and constant decomposition rate (Figure 2c) conditions corresponding to the thermal degradation of Vistalon7800. Valuable information can be extracted from the shape of the isothermal and constant decomposition rate curves. Firstly, the derivative of the isotherm shown in Figure 2b (dotted line) evidences an autoaccelerated process is

taking place; that is, the maximum reaction rate occurs not at the onset of the reaction but after it has already started. Such feature is characteristic of nucleation or chain scission driven reactions [24]. Likewise, the CRTA curve in Figure 2c displays a minimum in the T-α profile, also typical of nucleation or chain scission mechanisms [24]. These results clearly show that "n order" models are undoubtedly invalidated for describing the decomposition kinetics of EPDM because such models cannot at all reproduce an autoaccelerating behavior [25]. While not shown here, a similar conclusion was reached for the whole set of EPM and EPDM samples here investigated, regardless of its chemical composition.

Figure 3 shows the evolution of the activation energy with the extent of degradation process of the different EPM and EPDM samples, as calculated by means of the Friedman isoconversional method, described in section 3.2. There is no significant variation in the activation energy with the process progress, which supports that the degradation takes place through a single step process. Average values of activation energies as obtained by the Friedman analysis are included in Table 1 for all studied compositions. Figure 4 shows the results of the combined kinetic analysis of the degradation curves of Vistalon7800 appearing in Figure 2. The fitting of the experimental data to the Sestak-Berggren modified equation, as described in Section 3.3, results in all experimental data aligning when the *m* and *n* parameters take the values 0.418 and 1.013, respectively. The slope of the fit leads to an activation energy of 261.0±0.5 kJ $mol^{-1}$and the intercept to a preexponential factor of 3.8 10^{18}±0.3 10^{16} min^{-1}. It is noteworthy to point out the excellent agreement between this activation energy and those obtained for the same compound from the isoconversional method of Friedman, what supports the correctness of the kinetic analysis here outlined. It can be

observed that the error of the activation energy determined from combined kinetic analysis is considerably lower than the one obtained from the Friedman method. This behavior can be easily understood if we consider that the Friedman method takes a single point from every α-T plot for determining the activation energy at a given value of α while the combined method analyses at once the whole set of data obtained under different experimental conditions, leading to a considerably higher statistical weight. The master plot of the kinetic model obtained from this analysis, $\alpha^{0.418}(1-\alpha)^{1.013}$, is compared in Figure 5a with a set of kinetic models reported in the literature for describing solid state reactions. The whole set of plots are normalized at $\alpha = 0.5$ for a clearer comparison. It can be noticed how the deducted model resembles a chain scission kinetic model, confirming the observations made from the isothermal and constant rate curves in Figures 2b and 2c. In order to validate the kinetic parameters obtained from the analysis, a set of curves were simulated using a fourth order Runge-Kutta numerical integration method, assuming the aforementioned kinetic parameters and the experimental heating conditions used to obtain the experimental data. The simulations were performed using the Mathcad software (Mathsoft, Cambridge, MA, USA). Figure 2 shows the simulated curves match perfectly the experimental ones. The chain scission mechanism also explains previous findings by Gamlin, who detected the autoaccelerating nature of the EPDM degradation and found similarities with an Avrami-Erofeev two dimensional nucleation model [12, 19, 22]. As seen in Figure 5, both Avrami and chain scission are acceleratory models, but the latter underlying physical meaning is much more appropriate to a polymer degradation process. The fact that the thermal decomposition of these compounds follows a random scission kinetic model has important implications at a practical level. The initial induction period means that, if the material goes through a high temperature event during

processing, recycling or any application, the chain scission process will be already initiated and the degradation will speed up.

A similar analysis procedure was applied to the rest of the EPM and EPDM samples, reaching equivalent conclusions regarding the kinetic model. The activation energies, preexponential factors and *m* and *n* parameters corresponding to the *f(α)* kinetic models resulting from the kinetic analysis are included in Table 1. The full set of graphs showing the results of the analysis for each sample studied are included in the Supporting Information (Figs S1 to S24). In Figures 5b to 5f, the estimated *f(α)* kinetic models found for a selection of the tested elastomers are graphically compared with theoretical models. From these figures, it is clear that all processes can be attributed to a random scission model; in other words, the thermal decomposition of the whole set of samples here studied takes place through a mechanism that implies the random breakage of the polymer chain and the subsequent vaporization of the released fragments [25]. It is noteworthy to remark that it has been demonstrated for the first time in literature that the pyrolysis of EPM and EPDM takes place through a random chain scission mechanism. Considering the wide range of samples studied, differing in the ethylene/propylene ratios and in the type and quantity of diene, it can be assumed that they possess different polymer architectures due to varying crosslinking densities. It has been proposed that the degradation starts from a labile center; like a site of unsaturation or a tertiary carbon [22]. It has not been found a correlation between kinetic parameters of the pyrolysis of the EPDM samples and their composition, because a set of industrial samples have been used and there is not a systematic variation of the composition of the three components not even in the type of diene employed. Thus, the commercial samples incorporate two types of dienes, ENB and DCPD. Further studies using

synthesized samples of EPDM designed with a systematic variation of the composition would be required for clarifying the pyrolysis mechanism of these compounds. However, it is noteworthy to point out that the two EPDM samples that have practically the same composition, Vistalon7001 (manufactured by ExxonMobil) and EPDM70C2 (manufactured by DSM elastomers), have very close kinetic parameter for the pyrolysis, what suggests that the thermal stability of EPDM is exclusively depending on the composition of the polymer and is not influenced by particle size or other parameters depending of the processing method.

In the case of the EPM samples, which have no diene content and are exclusively constituted by ethylene and propylene, it is clearly noticeable a diminution of the activation energy with the increase of the percentage of propylene. This behaviour would be explained considering the higher vulnerability of the propylene molecule because of its tertiary carbon.

CONCLUSIONS

It has been demonstrated for the first time in literature that the pyrolysis of EPM and EPDM polymers fit a random scission kinetic model instead of a first order kinetics, independently of the chemical composition of the polymers, which means that the reaction rate is controlled by a random breakage of the polymer chain followed by the vaporization of the released fragments. It has been shown that, in the case of the binary copolymers constituted by ethylene and propylene (EPM), the activation energy clearly decreases by increasing the percentage of propylene in the polymer. This behavior has been explained as a function of the lower stability of the bond associated to the ternary carbon of polyethylene. It has not been possible to establish a clear correlation between the activation energy of the pyrolysis of EPDM samples and their composition because

of a lack of systematic variation in the composition of the industrial samples supplied that does not allow a systematic analysis. However, no significant changes of the activation energy with the composition of these terpolimers have been observed, although an increase of the stability as a function of the percentage of diene seems to be observed.

ACKNOWLEDGEMENTS

Financial support from project CTQ2011-27626 (Spanish Ministerio de Economía y Competitividad), Junta de Andalucía (TEP-7858) and FEDER funds are acknowledged. Additionally, one of the authors (PESJ) is supported by a Juan de la Cierva grant.

References

[1] Mark JE, Erman B, Eirich F. Science and Technology of rubber 3rd ed. Academic Press, 2005.

[2] Datta RN. Rubber Curing Systems. Shawbury, UK. Rapra Ltd., 2002.

[3] Ciesielski A. An Introduction to Rubber Technology. Shawbury, UK. Rapra Press, 1999.

[4] Morton M. Rubber Technology, Third Edition. London, New York1995.

[5] Aravind I, Albert P, Ranganathaiah C, Kurian JV, Thomas S. Compatibilizing effect of EPM-g-MA in EPDM/poly(trimethylene terephthalate) incompatible blends. Polymer 2004;45:4925-37.

[6] Chang YW, Yang YC, Ryu S, Nah C. Preparation and properties of EPDM organomontmorillonite hybrid nanocomposites. Polym. Int. 2002;51:319-24.

[7] Jiang W, Liu CH, Wang ZG, An LJ, Liang HJ, Jiang BZ, et al. Brittle-tough transition in PP/EPDM blends: Effects of interparticle distance and temperature. Polymer 1998;39:3285-8.

[8] Usuki A, Tukigase A, Kato M. Preparation and properties of EPDM-clay hybrids. Polymer 2002;43:2185-9.

[9] van der Wal A, Mulder JJ, Gaymans RJ. Polypropylene-rubber blends: 1. The effect of the matrix properties on the impact behaviour. Polymer 1998;39:6781-7.

[10] van der Wal A, Nijhof R, Gaymans RJ. Polypropylene-rubber blends: 2. The effect of the rubber content on the deformation and impact behaviour. Polymer 1999;40:6031-44.

[11] Wang XS, Luo N, Ying SK. Synthesis of EPDM-g-PMMA through atom transfer radical polymerization. Polymer 1999;40:4515-20.

[12] Gamlin C, Dutta N, Roy-Choudhury N, Kehoe D, Matisons J. Influence of ethylene-propylene ratio on the thermal degradation behaviour of EPDM elastomers. Thermochim. Acta 2001;367-368 185-93.

[13] Ghosh P CB, Sen AK. Thermal and oxidative degradation of PE-EPDM blends vulcanized differently using sulfur accelerator systems. Eur. Polym. J. 1996;32:1015-21.

[14] Zhao Q, Li X, Gao J, Jia Z. Degradation evaluation of ethylene–propylene–diene monomer (EPDM) rubber in artificial weathering environment by principal component analysis. Mater. Lett. 2009;63:116-7.

[15] Li J, Guo S, Li X. Degradation kinetics of polystyrene and EPDM melts under ultrasonic irradiation. Polym. Degrad. Stabil. 2005;89:6-14.

[16] De Paoli MA, Geuskens G. The Photo-oxidation of EPDM Rubber: Part I Kinetics of Oxygen Consumption. Polym. Degrad. Stabil. 1988;21 (1988):277-83.

[17] Guzzo M, De Paoli MA. The photo-oxidation of EPDM rubber: Part IV Degradation and stabilization of vulcanizates. Polym. Degrad. Stabil. 1992;36:169-72.

[18] da Costa HM, Ramos VD. Analysis of thermal properties and rheological behavior of LLDPE/EPDM and LLDPE/EPDM/SRT mixtures. Polym. Test. 2008;27:27-34.

[19] Gamlin C. Mechanism and kinetics of the isothermal thermodegradation of ethylene-propylene-diene (EPDM) elastomers. Polym. Degrad. Stabil. 2003;80:525-31.

[20] Assink RA, Gillen KT, Briana S. Monitoring the degradation of thermally aged EPDM terpolymer by ^{1}H NMR relaxation measurements of solvent swelled samples. Polymer 2001;43 (2002):1349-55.

[21] Zaharescu T, Meltzer V, Vilcu R. Thermal properties of EPDM/NR blends. Polym. Degrad. Stabil. 2000;70:341-5.

[22] Gamlin C, Markovic MG, Dutta NK, Choudhury NR, Matisons JG. Structural effects on the decomposition kinetics of EPDM elastomers by high-resolution TGA and modulated TGA. J Therm Anal 2000;59:319-36.

[23] Sanchez-Jimenez PE, Perejon A, Criado JM, Dianez MJ, Perez-Maqueda LA. Kinetic model for thermal dehydrochlorination of poly(vinyl chloride). Polymer 2010;51:3998-4007.

[24] Sanchez-Jimenez PE, Perez-Maqueda LA, Perejon A, Criado JM. Combined kinetic analysis of thermal degradation of polymeric materials under any thermal pathway. Polym. Degrad. Stabil. 2009;94:2079-85.

[25] Sanchez-Jimenez PE, Perez-Maqueda LA, Perejon A, Criado JM. A new model for the kinetic analysis of thermal degradation of polymers driven by random scission. Polym. Degrad. Stabil. 2010;95:733-9.

[26] Vyazovkin S, Dranca I, Fan XW, Advincula R. Kinetics of the thermal and thermo-oxidative degradation of a polystyrene-clay nanocomposite. Macromol Rapid Commun 2004;25:498-503.

[27] Sánchez-Jiménez PE, Pérez-Maqueda LA, Perejón A, Criado JM. Constant rate thermal analysis fot thermal stability studies of polymers Polym. Degrad. Stabil. 2011;96.

[28] Vyazovkin S, Sbirrazzuoli N. Isoconversional kinetic analysis of thermally stimulated processes in polymers. Macromol Rapid Commun 2006;27:1515-32.

[29] Vyazovkin S, Burnham AK, Criado JM, Perez-Maqueda LA, Popescu C, Sbirrazzuoli N. ICTAC Kinetics Committee recommendations for performing kinetic computations on thermal analysis data. Thermochim Acta 2011;520:1-19.

[30] Criado JM, Sanchez-Jimenez PE, Perez-Maqueda LA. Critical study of the isoconversional methods of kinetic analysis. J. Therm. Anal. Calorim. 2008;92:199-203.

[31] Perez-Maqueda LA, Criado JM, Malek J. Combined kinetic analysis for crystallization kinetics of non-crystalline solids. J Non-Cryst Solids 2003;320:84-91.

[32] Perez-Maqueda LA, Criado JM, Sanchez-Jimenez PE. Combined kinetic analysis of solid-state reactions: A powerful tool for the simultaneous determination of kinetic parameters and the kinetic model without previous assumptions on the reaction mechanism. J. Phys. Chem. A 2006;110:12456-62.

[33] Brown ME. Steps in a minefield - Some kinetic aspects of thermal analysis. J Therm Anal 1997;49:17-32.

Figure Captions.

Figure 1. Thermal degradation curves of the different EPM and EPDM samples studied in this work, recorded under a linear heating rate of 5 K min^{-1}. The plots show the reacted fraction as a function of the temperature. (a) EPDM and (b) EPM samples.

Figure 2. Vistalon7800 degradation curves, recorded under (a) linear heating rate, (b) isothermal and (c) constant rate experimental conditions. Curves represented by symbols correspond to the experimental curves whereas the solid lines correspond to the curves reconstructed assuming the kinetic parameters deduced from the combined kinetic analysis, that is, E= 261 $kJmol^{-1}$, A= 3.8 10^{18} and $f(\alpha)= \alpha^{0.418}(1-\alpha)^{1.013}$.

Figure 3. Activation energies as a function of the reacted fraction deduced for each elastomer. Values obtained by means of the Friedman isoconversional method.

Figure 4. Result of the Combined Kinetic Analysis for the case of the Vistalon7800 EPDM. The figure is obtained by plotting the left hand of Eq. (5) for every experimental curves in Figure 2 against the reverse of the temperature. The linear fit of such plot yields the kinetic parameters describing the process.

Figure 5. Comparison between some of the most usual ideal kinetic models and those deducted from the combined kinetic analysis for the degradation of (a) Vistalon 7800; (b) Vistalon 5601; (c) Vistalon 722; (d) EPDM 58%C2; (e) EPDM 70%C2 and (f) EPDM 49%C2

Table 1. List of the EP(D)M samples studied in this work. The weight percentage of ethylene and diene in the final polymer is included, as well as the type of diene employed(ENB stands for ethylidenenorbornene while DCPD stands for dicyclopentadiene). Temperatures corresponding to 10% (α=0.1, $\mathbf{T_{\alpha=0.1}}$) and 50% (α=0.5, $\mathbf{T_{\alpha=0.5}}$) degradation as obtained from Figure 1 (linear heating rate experiments at 5 K min^{-1}) are also displayed. Average activation energy values obtained by Friedman analysis and activation energy, preexponential factor and *n* and *m* parameters determined by combined kinetic analysis have also been incorporated.

	Sample	Ethylene Content (wt%)*	Type of diene and content (wt%)*	$T_{\alpha=0.1}$ (K)	$T_{\alpha=0.5}$ (K)	Friedman analysis	Combined kinetic analysis			
						Average Ea (kJ mol^{-1})	Ea (kJ mol^{-1})	Ln(A) Ln(min^{-1})	n	m
EPDM	Vistalon 5601	69.0	ENB 5.0	705.1	720.2	252±8	252±1	41.5±0.1	0.991	0.445
	Vistalon 7001	73.0	ENB 5.0	707	721.8	255±8	256±1	42.0±0.1	1.005	0.445
	Vistalon 7800	79.0	ENB 6.0	707	721.9	260±9	260±2	42.5±0.2	1.013	0.418
	EPDM 58 C2	58.0	DCPD 4.5	686.1	703.6	256±10	254±1	42.0±0.2	1.048	0.383
	EPDM 64C2	64.0	DCPD 1.0	697.6	716.5	250±10	251±1	41.3±0.1	0.971	0.38
	EPDM 67C2	67.0	ENB 4.3; DCPD 2.0	692.2	711.3	246±7	245±1	40.6±0.1	0.997	0.356
	EPDM 70C2	70.0	ENB 4.6	706.2	721,5	256±9	257±2	42.3±0.2	1.021	0.44
EPM	Vistalon 722	72.0	-	702.8	721,6	248±7	248±1	40.2±0.1	0.906	0.399
	EPM 49C2	49.0	-	682.4	712	230±9	230±1	37.6±0.1	0.871	0.268

*Balanced to 100% with propylene

FIGURE 1

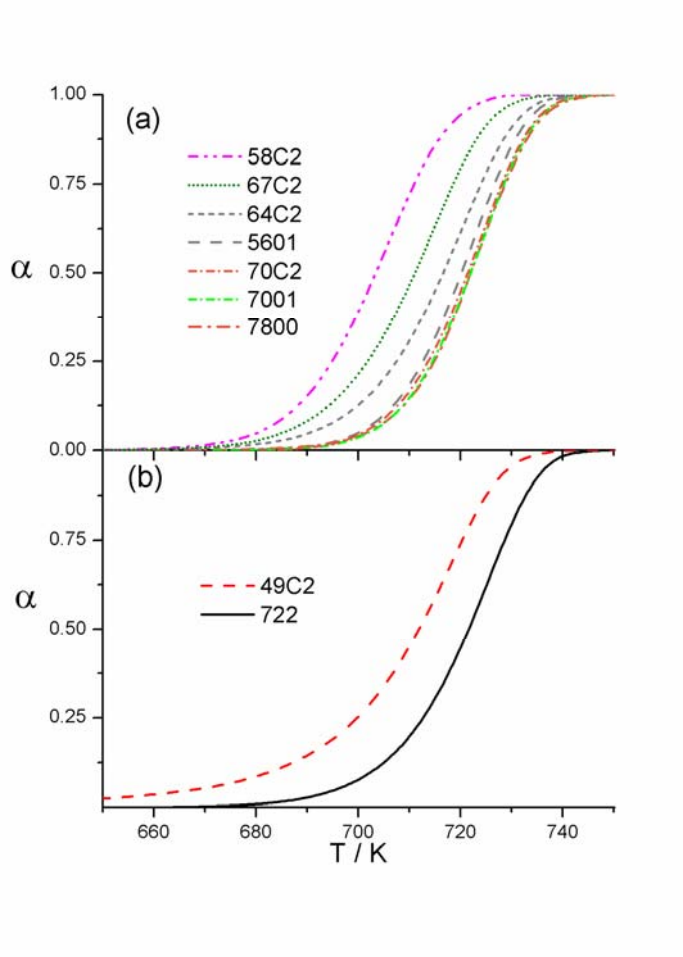

Figure 1. Thermal degradation curves of the different EPM and EPDM samples studied in this work, recorded under a linear heating rate of 5 K min^{-1}. The plots show the reacted fraction as a function of the temperature. (a) EPDM and (b) EPM samples.

FIGURE 2

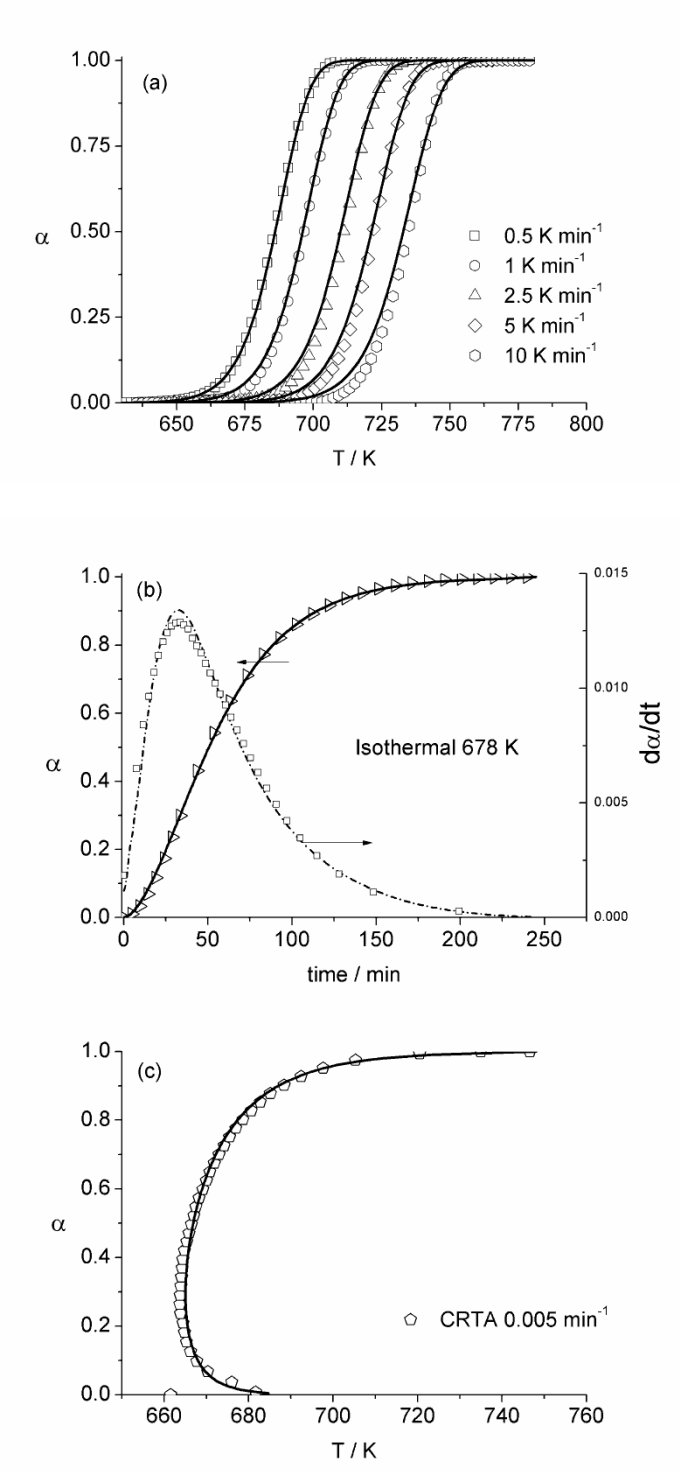

Figure 2. Vistalon7800 degradation curves, recorded under (a) linear heating rate, (b) isothermal and (c) constant rate experimental conditions. Curves represented by symbols correspond to the experimental curves whereas the solid lines correspond to the curves reconstructed assuming the kinetic parameters deduced from the combined kinetic analysis, that is, Ea= 261 kJmol^{-1}, A= 3.8 10^{18} and f(α)= $\alpha^{0.418}(1-\alpha)^{1.013}$.

FIGURE 3

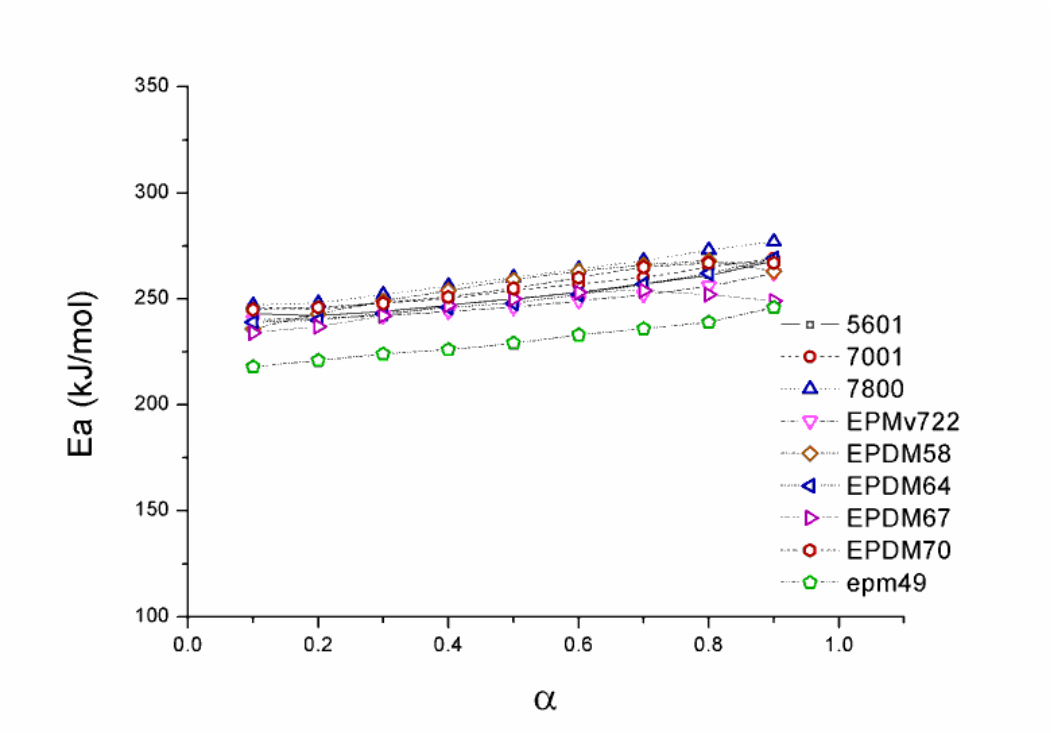

Figure 3. Activation energies as a function of the reacted fraction deduced for each elastomer. Values obtained by means of the Friedman isoconversional method.

FIGURE 4

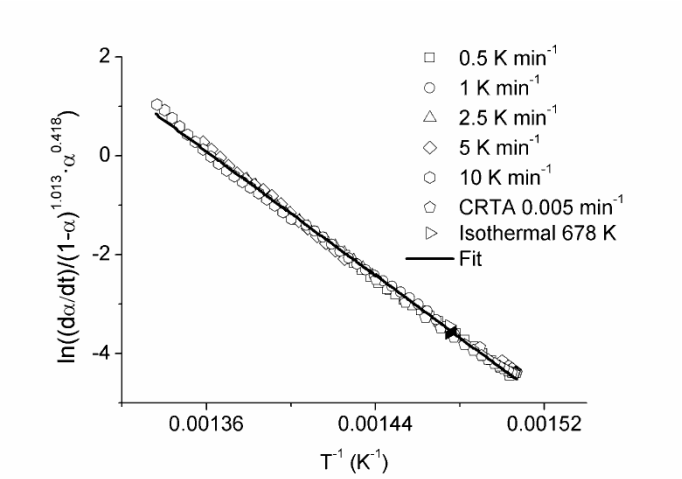

Figure 4. Result of the Combined Kinetic Analysis for the case of the Vistalon7800 EPDM. The figure is obtained by plotting the left hand of Eq (5) for every experimental curves in Figure 2 against the reverse of the temperature. The linear fit of such plot yields the kinetic parameters describing the reaction.

FIGURE 5

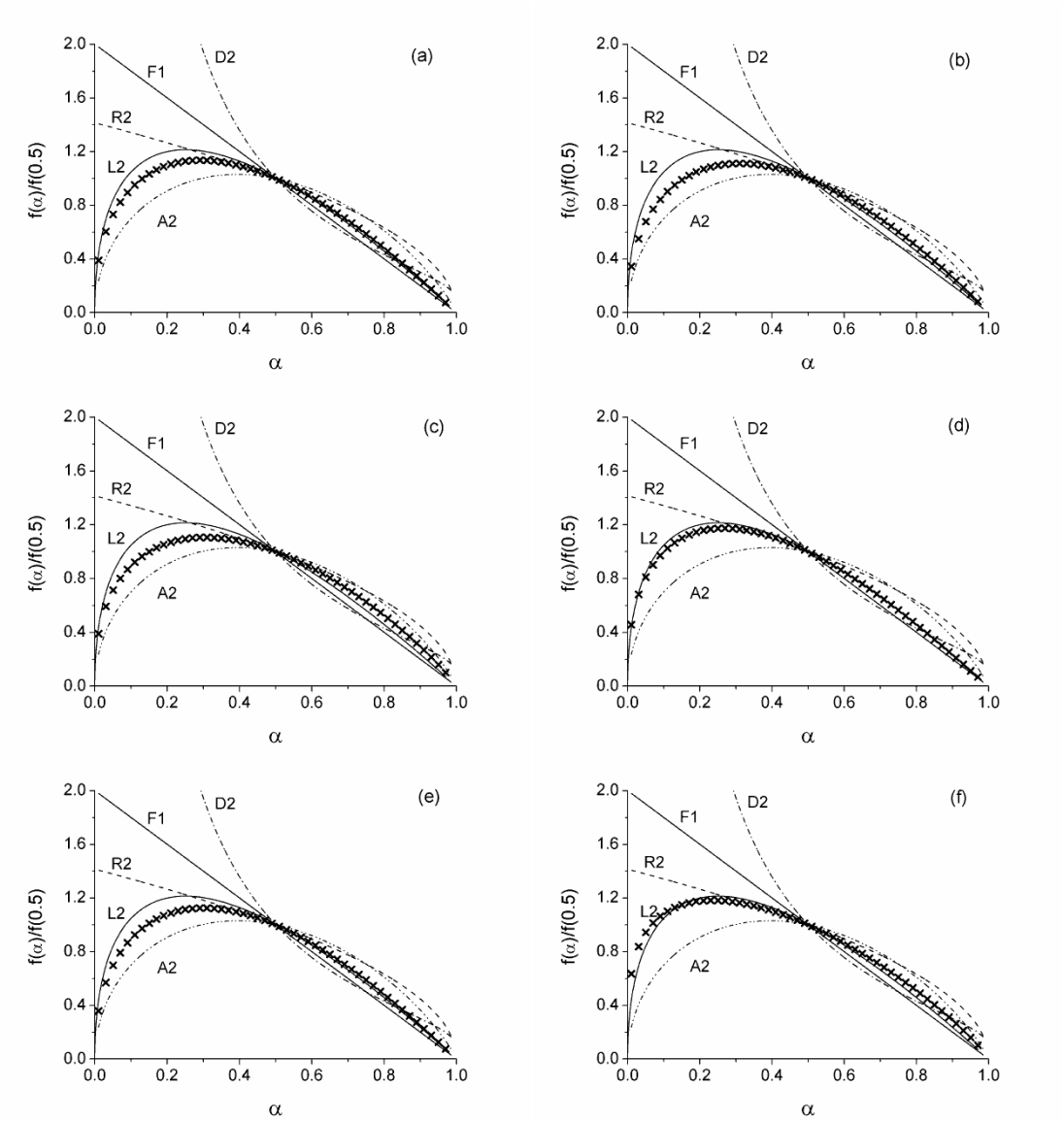

Figure 5. Comparison between some of the most usual ideal kinetic models and those deducted from the combined kinetic analysis for the degradation of (a) Vistalon 7800; (b) Vistalon 5601; (c) Vistalon 722; (d) EPDM 58%C2; (e) EPDM 70%C2 and (f) EPDM 49%C2